Electronic Supplementary Material (ESI) for Journal of Materials Chemistry A.

Amino-Functionalized Metal-Organic Framework achieving Efficient Capture-Diffusion-Conversion of CO_2 towards Ultrafast Li-CO_2 Batteries

Hu Hong,[a, b,] † Jiafeng He, [b] † Yanbo Wang,[a] Xun Guo,[a] Xiliang Zhao,[b] Xiaoke Wang,[b]

Chunyi Zhi [a,b] Hongfei Li,[b,c]* Cuiping Han, [d,]*

[a] *Department of Materials Science and Engineering, City University of Hong Kong, 83 Tat Chee Avenue, Kowloon, Hong Kong, 999077, China*

[b] *Songshan Lake Materials Laboratory, Dongguan, Guangdong, 523808, China*

c School of System Design and Intelligent Manufacturing, Southern University of Science and Technology, Shenzhen, 518055, China

[d] *Faculty of Materials Science and Energy Engineering / Low Dimensional Energy Materials Research Center, Shenzhen Institutes of Advanced Technology, Chinese Academy of Sciences, Shenzhen, 518055, China*

Email: lihf@sslab.org.cn; cp.han@siat.ac.cn

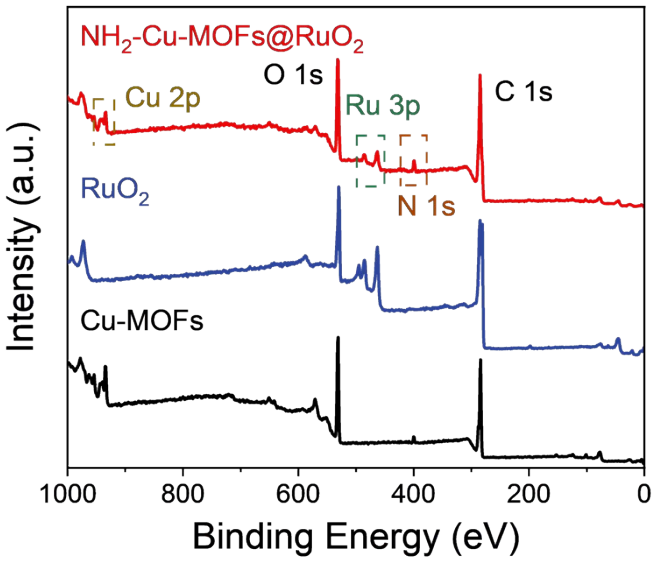

Figure S1. XPS survey spectra of NH_2-Cu-MOFs@RuO_2, RuO_2, and Cu-MOFs.

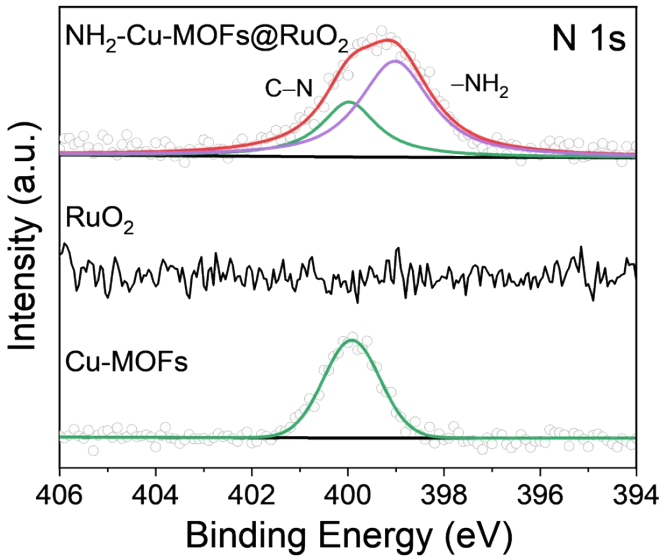

Figure S2. The high-resolution spectra of N 1s of NH_2-Cu-MOFs@RuO_2, RuO_2, and Cu-MOFs.

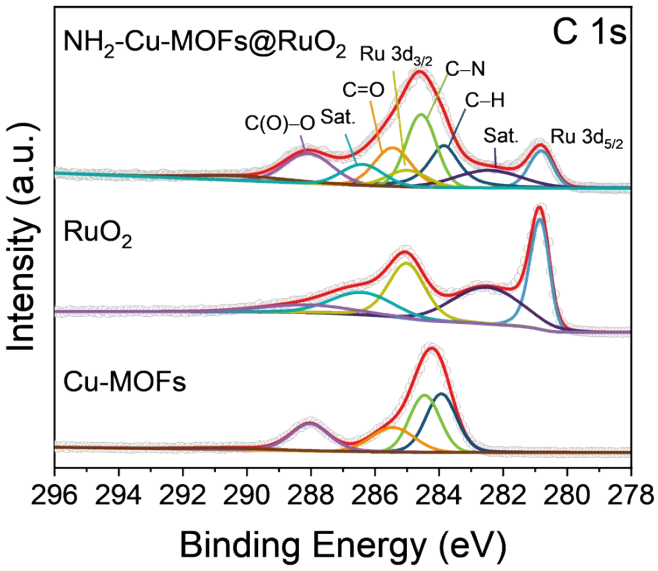

Figure S3. The high-resolution spectra of C 1s of NH_2-Cu-MOFs@RuO_2, RuO_2, and Cu-MOFs.

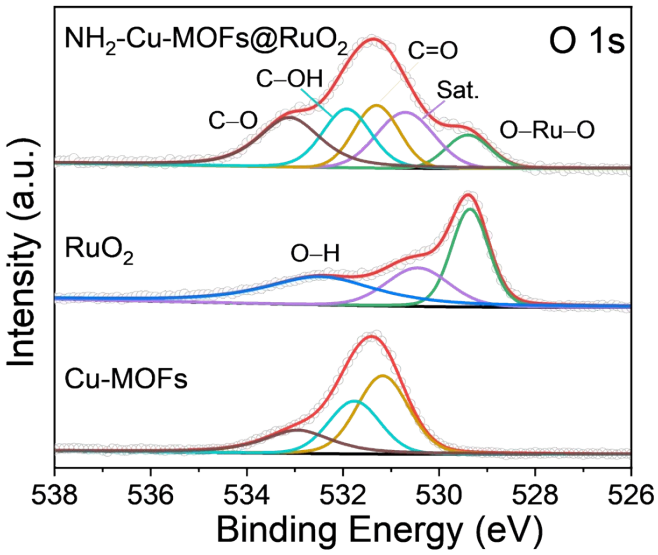

Figure S4. The high-resolution spectra of O 1s of NH_2-Cu-MOFs@RuO_2, RuO_2, and Cu-MOFs.

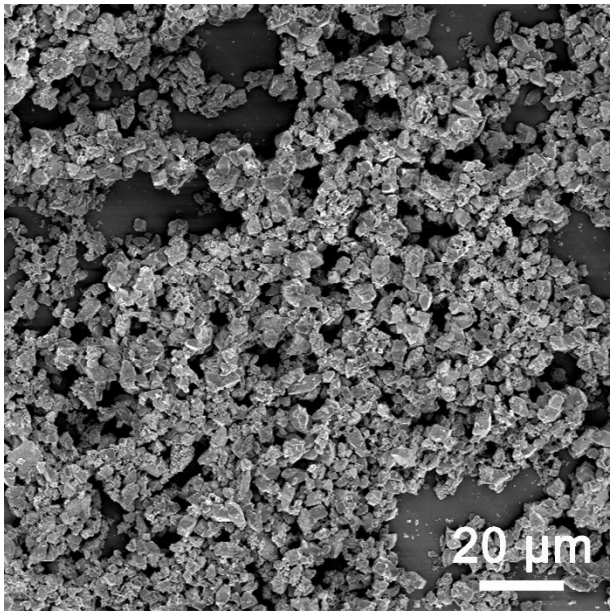

Figure S5. FESEM image of NH_2-Cu-MOFs@RuO_2.

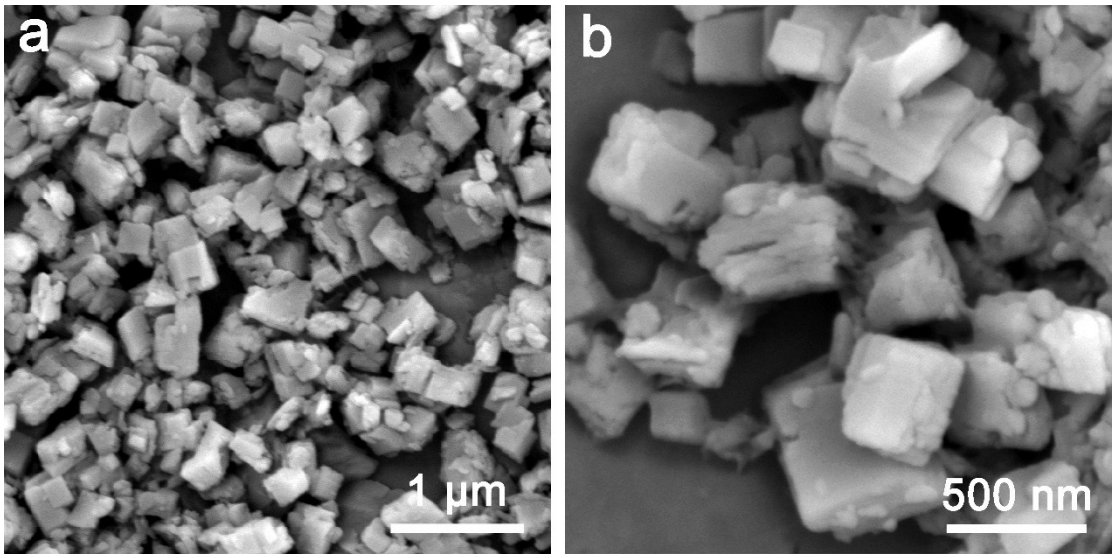

Figure S6. (a, b) FESEM images of Cu-MOFs at different magnifications.

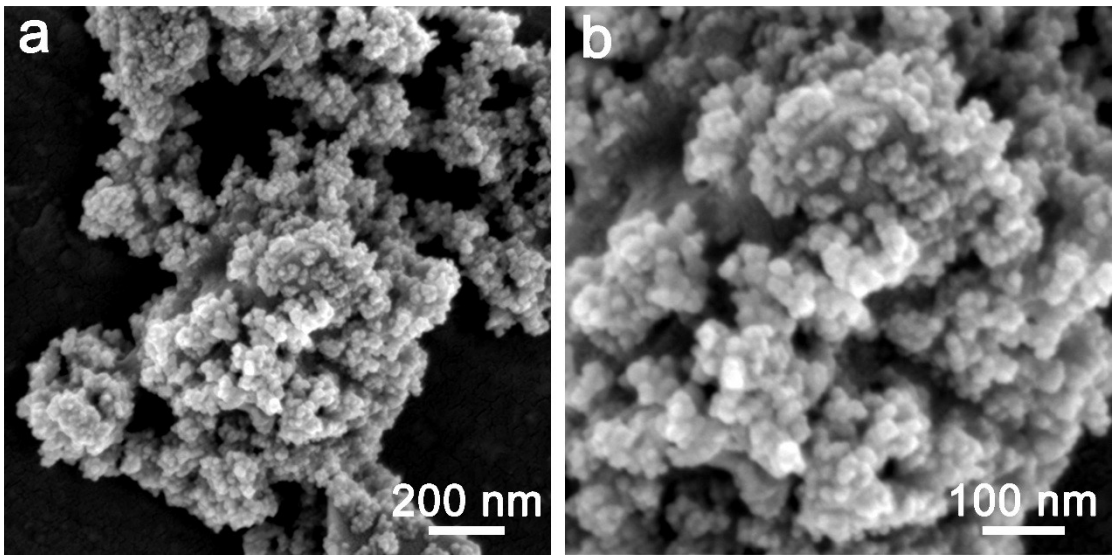

Figure S7. (a, b) FESEM image of RuO_2 at different magnifications.

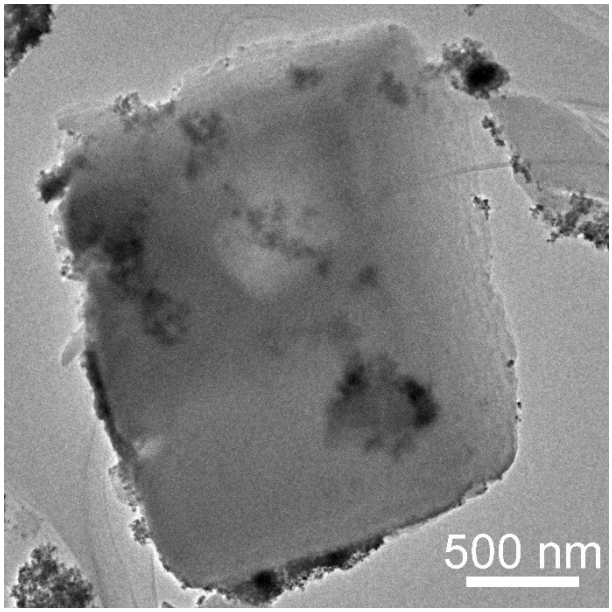

Figure S8. TEM image of the NH_2-Cu-MOFs@RuO_2.

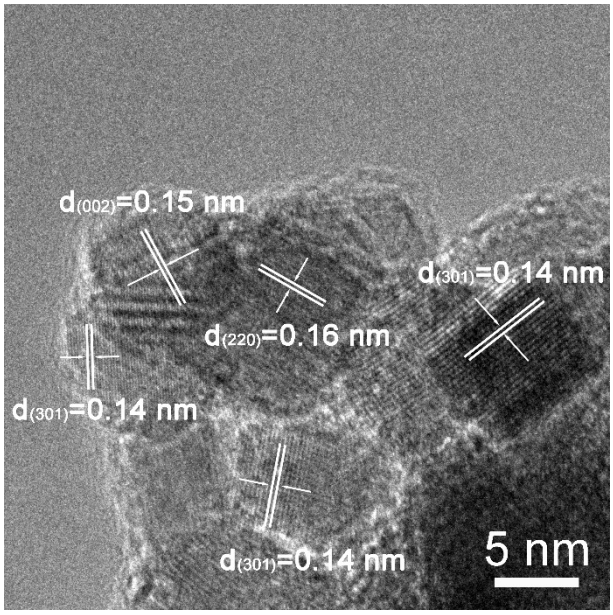

Figure S9. TEM image of RuO_2 inside NH_2-Cu-MOFs@RuO_2.

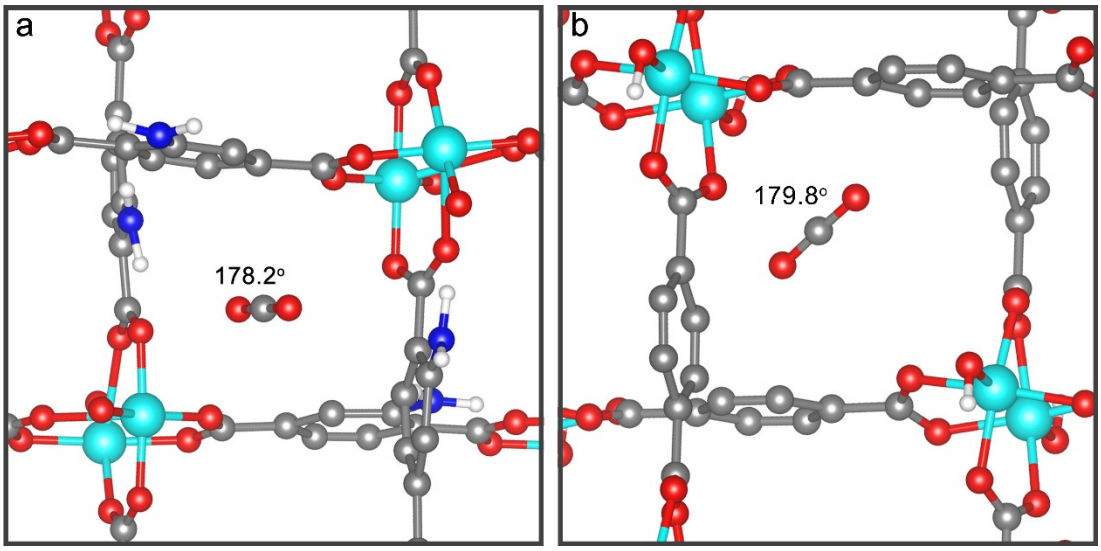

Figure S10. The simulation snapshots of (a) NH_2-Cu-MOFs@RuO_2 and (b) Cu-MOFs.

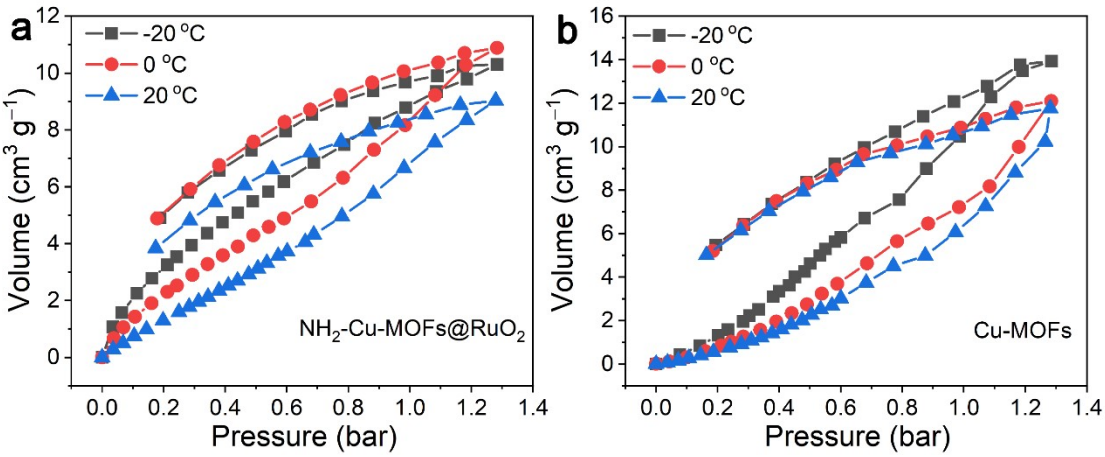

Figure S11. CO_2 sorption isotherms of (a) NH_2-Cu-MOFs@RuO_2 and (b) Cu-MOFs at 253, 273, and 293 K.

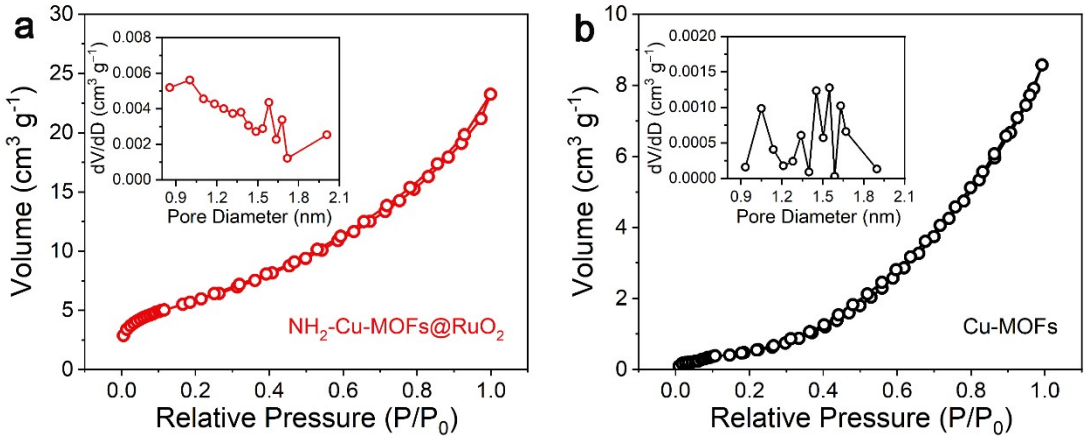

Figure S12. N_2 adsorption−desorption isotherms of (a) NH_2-Cu-MOFs@RuO_2 and (b) Cu-MOFs (inset shows corresponding micropore distributions, respectively).

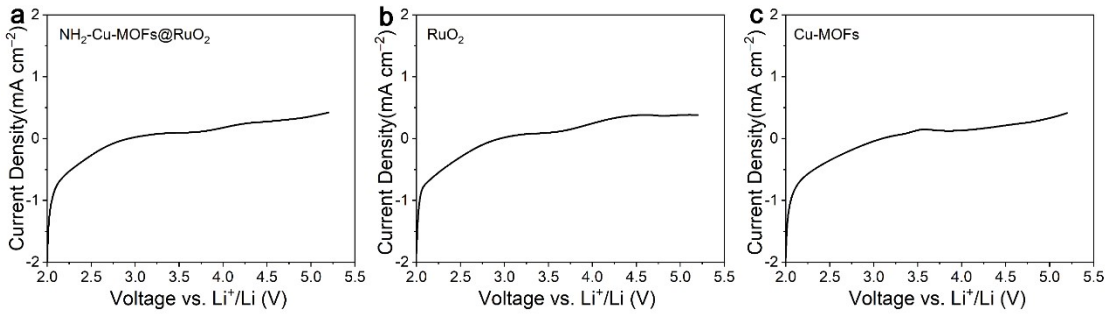

Figure S13. LSV curves of (a) NH_2-Cu-MOFs@RuO_2, (b) RuO_2, and (c) Cu-MOFs.

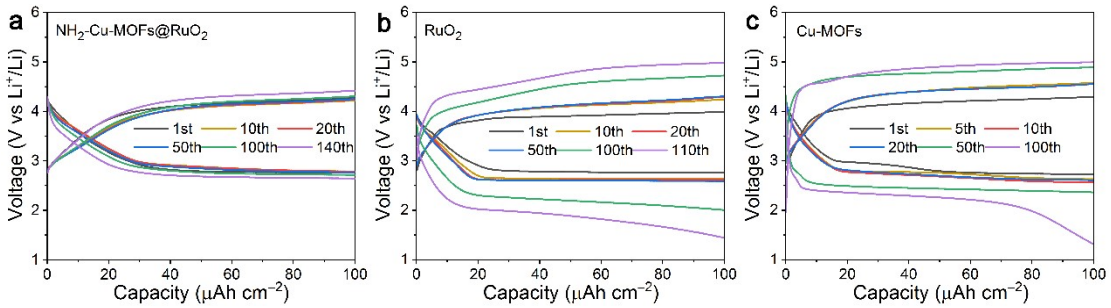

Figure S14. Charge-discharge curves of (a) NH_2-Cu-MOFs@RuO_2, (b) RuO_2, and (c) Cu-MOFs.

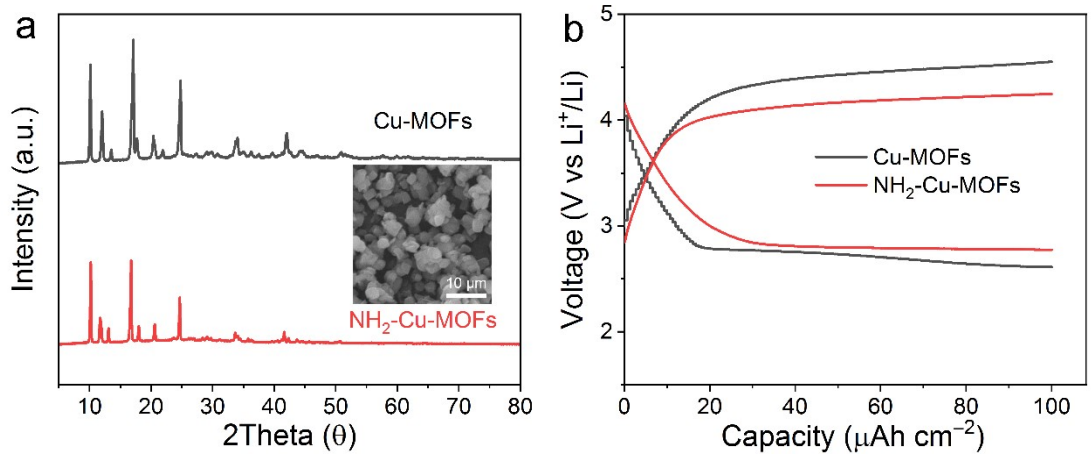

Figure S15. (a) XRD pattern of Cu-MOFs and NH_2-Cu-MOFs. (b) Charge-discharge curves of Cu-MOFs and NH_2-Cu-MOFs within a limiting capacity of 100 μA h cm^{-2} at a current density of 50 μA cm^{-2}.

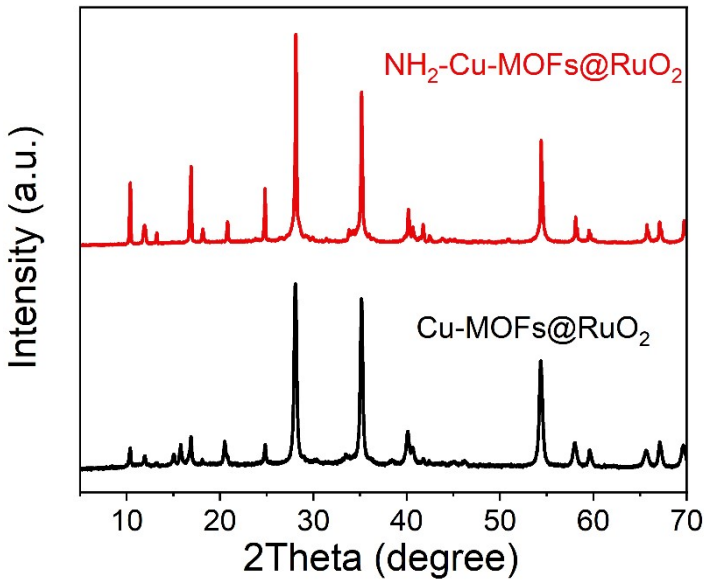

Figure S16. Comparison of XRD pattern of NH_2-Cu-MOFs@RuO_2 and Cu-MOFs@RuO_2.

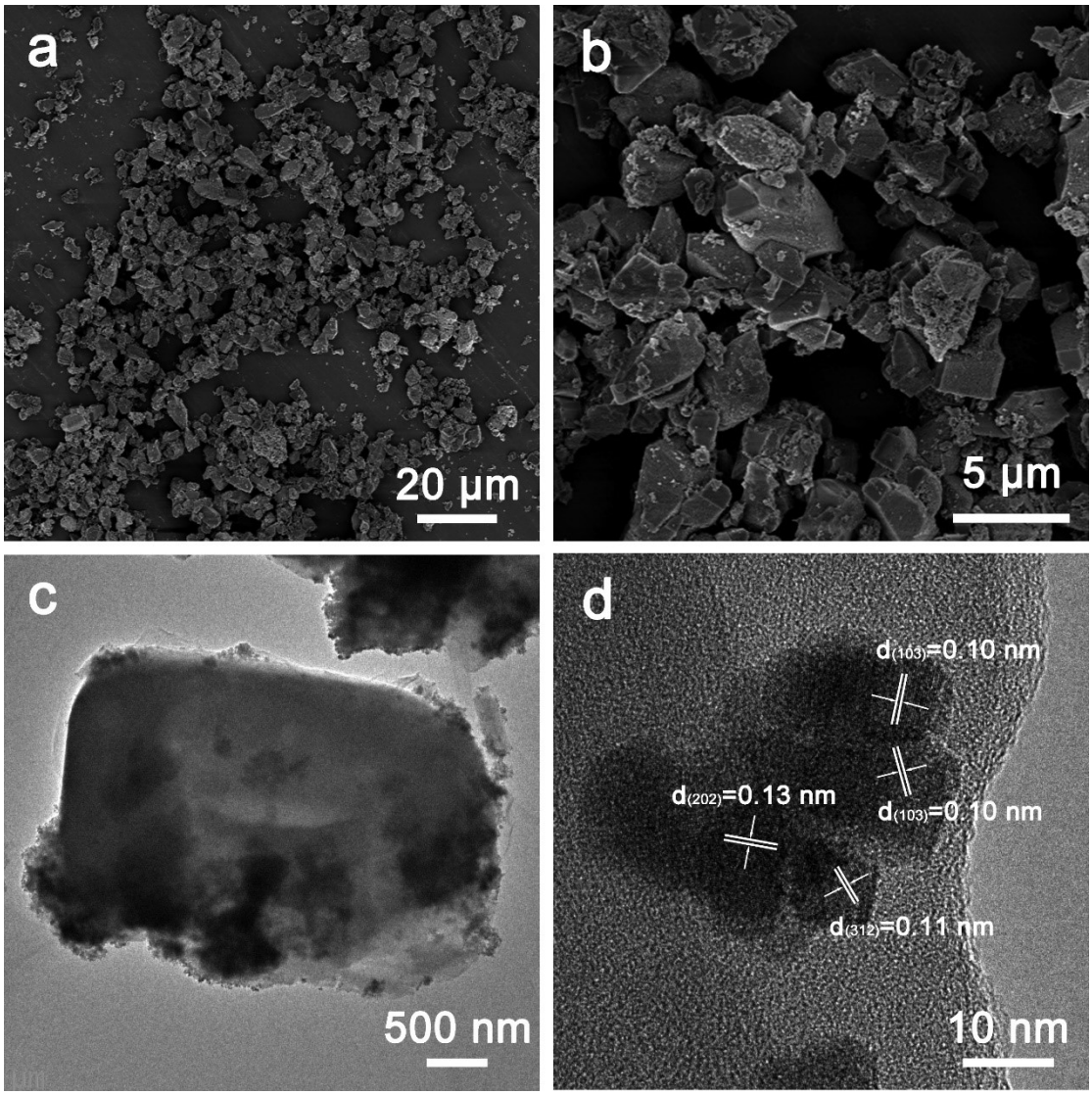

Figure S17. (a, b) FESEM images of Cu-MOFs@RuO_2 at different magnifications. (c) TEM and (d) HRTEM images of Cu-MOFs@RuO_2.

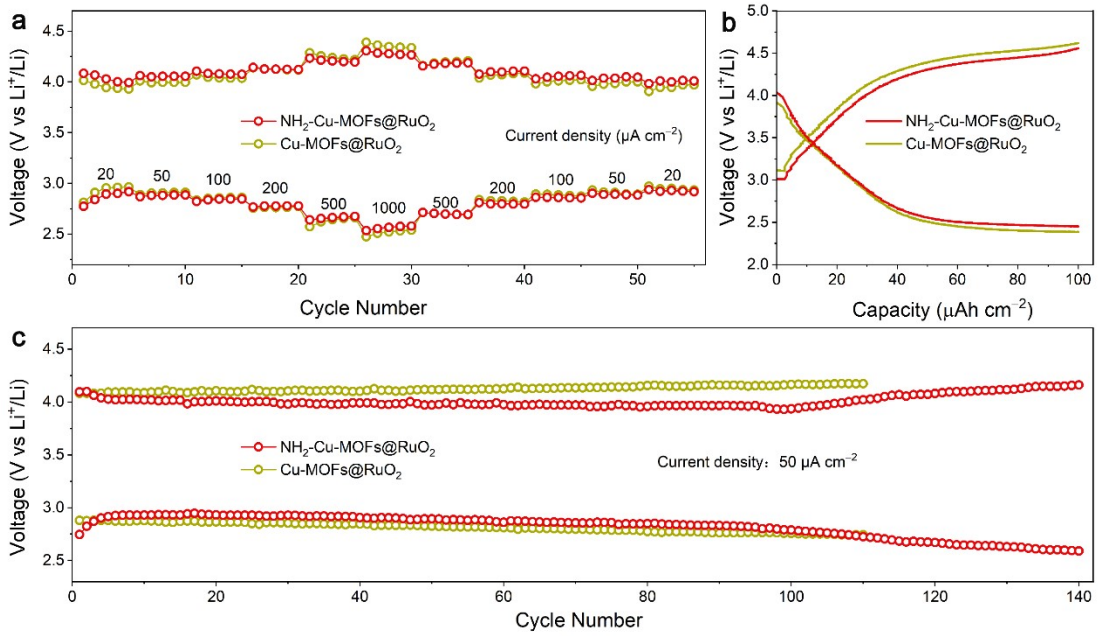

Figure S18. The electrochemical performances of Li–CO_2 batteries with NH_2-Cu-MOFs@RuO_2 and Cu-MOFs@RuO_2 cathodes. (a) Rate performances within a limiting capacity of 100 μA h cm^{-2} at various current densities. (b) Charge-discharge curves within a limiting capacity of 100 μA h cm^{-2} at a current density of 1000 μA cm^{-2}. (c) Cycle performance at a current density of 50μA cm^{-2}.

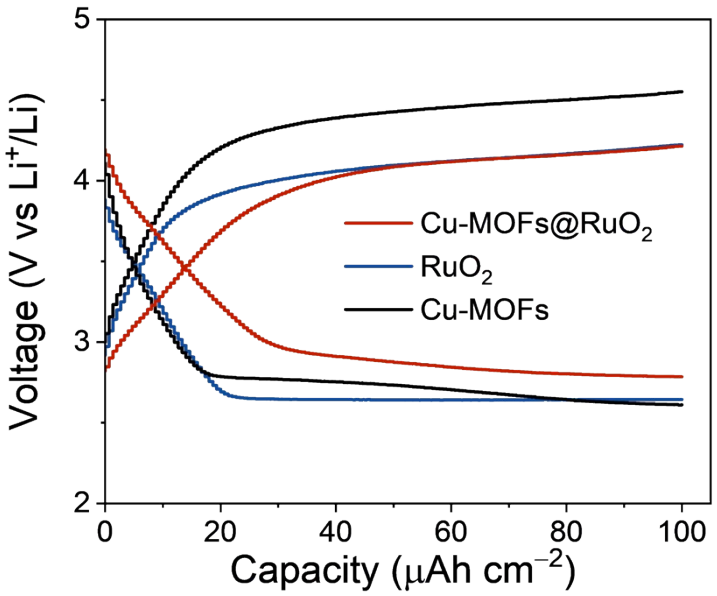

Figure S19. Charge-discharge curves of Cu-MOFs@RuO_2, RuO_2, and Cu-MOFs within a limiting capacity of 100 μA h cm^{-2} at a current density of 50 μA cm^{-2}.

Table S1. The R_s and R_{ct} values of NH_2-Cu-MOFs@RuO_2, RuO_2, and Cu-MOFs.

Sample	R_s (Ω)	R_{ct} (Ω)
NH_2-Cu-MOF@RuO_2	34.5	70.0
RuO_2	36.4	107.2
Cu-MOF	762.2	254.7

Table S2. Performance comparison of different Li-CO_2 batteries reported in the literature.

Cathode catalast	Current density (mA g^{-1})	Cutoff capacity (mAh g^{-1})	Recyclability (cycles)	References
NH_2-Cu-MOF@RuO_2	100	200	140	This work
RuO_2	100	200	111	This work
Cu-MOF	100	200	100	This work
CC@Mo_2C NPs	20	100	20	Ref. 1
0.25 M PDS	22	56	30	Ref. 2
CNT@C_3N_4	500	500	100	Ref. 3
MnO@NMCNFs (MOF)	36	452	52	Ref. 4
Gu-NG	200	1000	50	Ref. 5
Ru-Cu-G	400	1000	100	Ref. 6
Ru(II) catalyst	300	1000	60	Ref. 7
Li_2MnO_3	500	1000	30	Ref. 8
$Mn(HCOO)_2$ (MOF)	200	1000	50	Ref. 9
Mn_2(dobdc) (MOF)	200	1000	50	Ref. 10
MnTPzP-Mn (MOF)	200	1000	90	Ref. 10

Reference

1. J. Zhou, X. Li, C. Yang, Y. Li, K. Guo, J. Cheng, D. Yuan, C. Song, J. Lu and B. Wang, Adv. Mater., 2019, 31, 1804439.

2. R. Pipes, A. Bhargav and A. Manthiram, Adv. Energy Mater., 2019, 9, 1900453.

3. J. Li, K. Zhang, Y. Zhao, C. Wang, L. Wang, L. Wang, M. Liao, L. Ye, Y. Zhang, Y. Gao, B. Wang and H. Peng, Angew. Chem. Int. Ed., 2022, 61, e202114612.

4. S. Li, Y. Liu, X. Gao, J. Wang, J. Zhou, L. Wang and B. Wang, J. Mater. Chem. A, 2020, 8, 10354-10362.

5. Z. Zhang, Z. Zhang, P. Liu, Y. Xie, K. Cao and Z. Zhou, J. Mater. Chem. A, 2018, 6, 3218-3223.

6. Z. Zhang, C. Yang, S. Wu, A. Wang, L. Zhao, D. Zhai, B. Ren, K. Cao and Z. Zhou, Adv. Energy Mater., 2019, 9, 1802805.

7. Zhang, Z.; Bai, W.-L.; Cai, Z.-P.; Cheng, J.-H.; Kuang, H.-Y.; Dong, B.-X.; Wang, Y.-B.; Wang, K.-X.; Chen, J.-S., Enhanced Electrochemical Performance of Aprotic Li-CO_2 Batteries with a Ruthenium-Complex-Based Mobile Catalyst. *Angew. Chem. Int. Ed.* **2021,** *60* (30), 16404-16408.

8. Z. Zhuo, K. Dai, R. Qiao, R. Wang, J. Wu, Y. Liu, J. Peng, L. Chen, Y.-d. Chuang, F. Pan, Z.-x. Shen, G. Liu, H. Li, T. P. Devereaux and W. Yang, Joule, 2021, 5, 975-997.

9. S. Li, Y. Dong, J. Zhou, Y. Liu, J. Wang, X. Gao, Y. Han, P. Qi and B. Wang, Energy & Environmental Science, 2018, 11, 1318-1325.

10. L.-Z. Dong, Y. Zhang, Y.-F. Lu, L. Zhang, X. Huang, J.-H. Wang, J. Liu, S.-L. Li and Y.-Q. Lan, *Chem. Commun.*, 2021, **57**, 8937-8940.